Original Article

Size Control of Ag Nanoparticles Synthesized by PLA Method in Different Liquid Environments and their Potent against Virulent Candida Albicans

Salma. S. Abdullah[1], Sabah. A. Salman[2], A. Kadhim[3], Azhar. M. Haleem[4]

[1]Student, Department of Physics, College of Science, University of Diyala, General Directorate of Education Diyala, Iraq. E-mail: dr.salmaalshamari@gmail.com

[2]Professor, Department of Physics, College of Science, University of Diyala, Iraq. E-mail: pro.dr_sabahanwer@yahoo.com

[3]Professor, Department of Laser and Optoelectronics Engineering, University of Technology, Iraq. E-mail: abdulhadi.k.judran@uotechnology.edu.iq.

[4]Assistant Professor, Environment Research Center, University of Technology, Iraq. E-mail: amhjanabi74@gmail.com

Abstract

Human candidiasis is mostly caused by *Candida albicans*. It is now one of the most prevalent, recurrent and drug resistant forms of fungal infection, especially vaginal candidiasis. This research examined the antifungal activity of silver nanoparticles $AgNP_s$ on the viability of *C. albicans*. Pulsed laser ablation was used to produce silver nanoparticles in liquids in diverse liquid environments, with a Nd-YAG laser pulsed Q-switched wavelength (1064nm), number of pulses about (1000) pulses, and the repetition rate of (1)Hz. UV-VIS and TEM techniques were used to determined the optical and morphological properties of the produced colloidal nano-solutions. UV-VIS exhibited a characteristic peak at the site of the surface plasmon peak (SPR) at (400 nm) in double deionized distilled water (DDDW), and this value increased to (407, 408 and 415 nm) when used the solutions (SDS, CTAB and $NaBH_4$), respectively. The morphological properties TEM of Ag NP_s were distinguished, including particle size and shape where indicating that the shapes of spherical nanoparticles are heterogenic with an average size ranging (41.198- 50.631) nm. In addition, the current investigation revealed that $AgNP_s$ possess excellent and considerable antifungal activity, and that the rate of inhibition of *C. albicans* gradually increases as concentrations rise. The genotoxicity indicated a decrease in values of (BI), (MI) with increases concentrations. This drop is attributable to the interaction of (NP_s) with cellular structures. While the value of (TCA) only slightly rose at concentration (75µg/mL), it was demonstrated that silver nanoparticles could change cell structure.

Keywords: Silver Nanoparticles, UV-VIS, TEM, *Candida albicans.*

Received date: 24 August 2022 **Accepted: 28 September, 2022** **Published: 07 October, 2022**

DOI:10.47750/pnr.2022.13.04.054

INTRODUCTION

Candidiasis is one of the most common infections on a global scale. *Candida spp.* are responsible for various forms of dermal and systemic pathogenesis. *C. albicans* is a dimorphic opportunistic microorganism. It is found in the gastrointestinal, respiratory, and genitourinary tracts as a habitat microflora. Normally harmless, it may change into an opportunistic pathogen in immunocompromised or immunodeficient individuals [1-3]. *C. albicans* is the most common cause of oral, vaginal and skin infections (>90%) [2,4,5]. The frequency of *C. albicans* isolated in candidemia is of (46.3%), followed by *C. glabrata* (24.4%) [3,6]. Pulsed laser ablation in liquid is a quick, easy, and non-catalyzed approach to creating new materials. Nano-sized metal particles in a colloidal solution [7,8]. Ablation of a metal target immersed in a liquid medium using high-power laser energy involves adjusting laser settings such as laser wavelength, laser pulse duration, and so on to optimize productivity and NP_s particle size [9,10]. Dimensions, shape, concentration, solubility and surface charge, stability and a wide surface area are all benefits of NP_s, all of which contribute to their antibacterial characteristics. It is the minor NP_s small size and high surface-to-volume ratio that set them apart. The primary reasons why it is effective as an antibacterial agent. The metal NP_s are similar in size to the because metal NP_s are smaller than most biological molecules, they can easily pass through the cellular membrane of the harmful bacterium [11]. Because of their antimicrobial properties, silver nanoparticles (SN) have been extensively studied during the last two decade.

Nanoparticles are smaller in size, have a greater surface area-to-volume ratio, and have a bigger surface area available for contact with microorganisms than micro particles [12]. Silver nanoparticles bind to sulphur-containing proteins in biological molecules, causing microbial cell membrane abnormalities and intracellular content loss. The nanoparticles inside the cells hinder respiratory chain enzymes, causing microbial cells to die. Furthermore, silver nanoparticles can attach to phosphorus-containing molecules such as DNA, limiting cell replication [12,13]. These nanoparticles, for example, were added into acrylic resin to prevent denture stomatitis [14]. When new engineering technologies are used on silver nanoparticles $AgNP_s$, they end up with very different shapes and properties. Silver is made into very small pieces that are usually between 1 and 100 nm [15]. At the nanoscale, the ultrasmall size of particles leads to an extremely large surface area per mass. This means that a lot of atoms are in direct contact with the environment and ready to react. Certain sizes and shapes of silver nanoparticles have been shown to have different effects on different types of pathogens [16].

Moreover, studies have revealed that they have antibacterial effects, although it is not known how effective nano-Ag is against cutaneous fungal diseases. In this study we investigated the impact of $AgNP_s$ produced in (DDDW) along with surfactants like (SDS, CTAB and $NaBH_4$), and we came to the conclusion that we are able to manufacture $AgNP_s$ with a high density and a small size about (50 nm) within the nano-scale and almost spherical shapes. Because of its small size and spherical shape, it showed an inhibitory effect high against yeast (*C. albicans*) isolated from (vaginal candidiasis).

Experimental Section

2.1 Materials

With the aid of an energy dispersive X-ray fluorescence (ED-XRF) device (model XEPOS), the purity of a silver plate was determined to be 98.99%, as shown in the table (1) and figure (1). Other liquids tested included double deionized distilled water (DDDW), sodium dodecyl sulfate (SDS), which has the chemical formula is $NaC_{12}H_{25}SO_4$ (Kanto Chemical Co., Inc.), 96% purity and M.W = 288.372 g/mol, cetyltrimethylammonium bromide (CTAB), (99.5 %, Evans UK, the chemical formula is $C_{19}H_{42}BrN$ with M.W = 364.45 g/mol and sodium bromide borohydride ($NaBH_4$), the chemical formula is $NaBH_4$ (Kanto Chemical Co., Inc.), > 96% purity and M.W = 37.83 g/mol.

2.2 Synthesis of Silver NPs

Silver target was conducted to pulsed laser ablation (PLA) in liquid. Briefly, a silver plate of thickness (2mm) and dimensions (1cm x 1cm) was used as the target material. It was washed based on deionized ethanol and acetone and then polished with sandpaper to remove surface impurities. Then the plate is placed at the bottom of a glass container of (Pyrex) where the plate is immersed in different aqueous solutions, which are a solution of highly purified deionized water (DDDW), solutions of deionized water mixed with surfactants (SDS, CTAB and $NaBH_4$), at room temperature, a Q-switched pulsed Nd:YAG laser was used to focus on the plate that was in liquid. Table (2) gives a brief overview of the laser beam's parameters, figure (2) shows a diagram of how the experiment was set up. In all of the experiments, the fluid level was (2 mm) above the surface of the target.

Table (1): Silver plate analysis by XRF

Symbol	Element	Concentration	Abs error
Mg	Magnesium	0.0022 %	0.0 %
Al	Aluminum	0.0040 %	0.0 %
Si	Silicon	0.0013 %	0.0 %
P	Phosphorus	0.0030 %	0.0 %
S	Sulfur	0.0020 %	0.0 %
Ti	Titanium	0.0013 %	0.0 %
V	Vanadium	0.0015 %	
Cr	Chromium	0.0094 %	
Mn	Manganese	0.0065 %	0.0015 %
Fe	Iron	0.0934 %	0.0 %
Co	Cobalt	0.0031 %	0.0 %
Ni	Nickel	0.0084 %	0.0022 %
Cu	Copper	0.3726 %	0. 0048 %
Zn	Zinc	0.0416 %	0.0018 %
As	Arsenic	0.00508 %	0.00087 %
Zr	Zirconium	0.0050 %	0.0 %
Nb	Niobium	0.014 %	0.0 %
Mo	Molybdenum	0.019 %	0.0061 %
Ag	Silver	98.16 %	0.15 %
Cd	Cadmium	0.0624 %	0.0082 %
Sn	Tin	0.058 %	0.0 %
Sb	Antimony	0.0043 %	0.0 %
W	Tungsten	0.0035 %	0.0030 %
Pb	Lead	0.1482 %	0.0027 %
Sum of concentration 98.99 %			

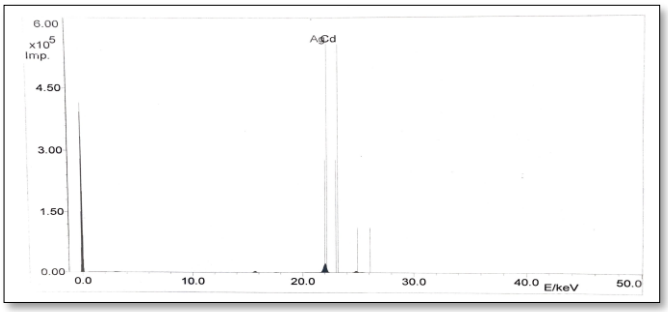

Figure (1): X-ray fluorescence spectrum of silver plate

Table (2): The details of Nd:YAG laser beam parameters

Laser Parameters	Characterizations
Wavelength	1064nm/532nm/1320nm
Laser energy	20-2000mJ
Pulse duration	10ns
Repetition rate	Maximum 10Hz
Spot size	1-8mm

Focal length of the lens	10cm

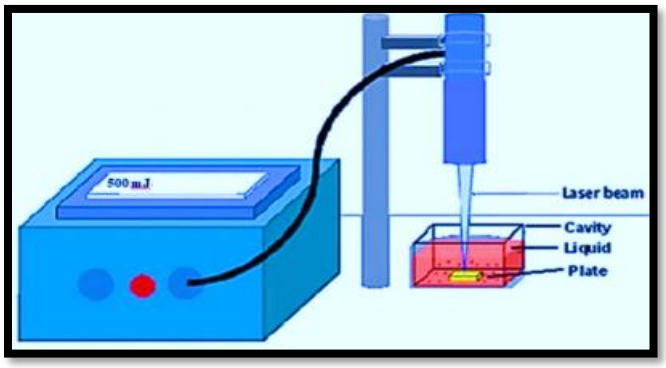

Figure (2): Schematic diagram of PLAL for NPs synthesized

2.3 Candida albicans Isolate

One multi-drug resistant pathogenic isolate of *C. albicans* was obtained from a postgraduate laboratory at the Baghdad University College of Science. This isolate was conserved, maintained, and utilized throughout the duration of the study to examine the antimicrobial effects of the produced nanoparticles on its viability and activity.

2.3.1 Antimicrobial Activity Assay

The antimicrobial activities of *C. albicans* that had been pre-activated for (24 hrs) at (37º C) in nutrient broth, the cell suspension containing ($1x10^6$ CFU/mL). The well diffusion method was used on the solid surface Muller Hinton agar with inoculated with (100µL) of candida cell suspension, six wells with a diameter of (6mm), was filled with (100µL) of different concentrations of nanoparticles prepared by laser ablation and different solvents (0.0, 25, 50, 100 and 200) µg/mL, and incubating for (24 hrs) at (37º C). The inhibitory zone diameter was estimated and reported as the experiment's (mean ±standard deviation) for three replicate of each treatment. The inhibition rate (percent) of tested *C albicans* was determined as follows [17]:

$$\text{Inhibition rate (\%)} = \left(\frac{Control-Test}{Control} \times 100\%\right) \quad \ldots\ldots\ldots\ldots\ldots\ldots\ldots (1).$$

2.4 Cytogenetic Study of Ag NPs

Chromosomal analysis for peripheral blood lymphocytes (PBL) was done in accordance with [18] by culturing (0.5mL) millimeters of heparinized venous blood from healthy persons, unexposed to any types of pollution, nonsmokers, with age from (25-35) years old. Chromosomal analysis were conducted by mixing (0.5mL) of peripheral blood to (4.5mL) of tissue culture media (RPMI-1640) supplied with (15%) of fetal bovine serum, and (10 µg/mL) of phytohemagglutinin (PHA) with different concentrations of prepared AgNPs (0.0, 25, 50, 100, and 200) µg/mL, and one concentration of Mitomycin-C MMC (0.65) µg/mL as a positive control. after (70 hrs) of incubation in (5% CO_2) at (37º C), we supplement the culture with (10µg/mL) of Colchicine solution to all test tubes and re-incubated at (37º C) for two hours, after that all tubes were centrifuged at (3000g) for (5 min), the pellet were mixed with (5 mL) of hypotonic solution (KCl) and returned to the incubator for (20 min) at (37º C). then we neglected the supernatunt by centrifugation at (3000g) and re-suspended the pellet with an identical volume of cool fixative solution (3:1 volume to volume of absolute methanol and glacial acetic acid), the final solution was added drop wise with continuous mixing, with repeating this step three times, we take the transparent white pellet of lymphocytes, which was dropped over clean, iced glass slides. Blastogenic index (BI) was measured in (1000) stimulated cells, and Mitotic Index (MI) also determined as shown in the following equation [19]:

$$\text{MI= Mitotic cells/ 1000 cells} \times 100\ \% \quad \ldots\ldots\ldots\ldots\ldots\ldots\ldots\ldots\ldots\ldots (2)$$

While the total chromosomal aberrations (TCA) calculated in (25) very well metaphase.

2.5 Characterization Techniques

UV-VIS spectroscopy (Double Beam 1800 UV Spectrometer) was used to record absorption spectra and surface plasmon resonance (SPR) for colloids (Shimadzu, Japan). A transmission electron microscope (TEM) model (ZEISS LED 912 AB-100KV, Germany) has been used to investigate the morphological features of Ag nanoparticles.

2.6 Statistical Analysis

All data were analyzed by two way analysis of variance (ANOVAI) by using SPSS software version 22, and recorded as (Mean ± Standard deviation) for three replicates of each experiments, and the least significant differences (LSD) calculated at $p < 0.05$.

Results and Discussions

3.1 UV-VIS Analysis and Energy Gap Calculation

A colloidal solution containing silver nanoparticles targeted by the liquid pulse laser ablation method, was prepared to study the effect of different solutions on the properties and size of nanoparticles at constant energy (500 mJ), number of pulses (1000) and wavelength (1064 nm). Table (3) shows the surface plasmon peak (SPR) location of the silver nanoparticles. Figure (3) shows the absorption spectrum of the silver nanoparticles solution, where we observe the peak of the surface flour peak around (400nm) and this indicates that the prepared nanoparticles are almost spherical [20]. The peak intensity increase in all the NP-containing solutions with surfactants compared with that with DDDW indicates an increase in the production efficiency of the $AgNP_s$ [21]. The chemical bonds of its constituent elements and the size of the molecules have a significant impact on

the energy gap, and in general, the energy gap (Eg) changes with the change in particle size, as evidenced by the values of the energy gap in table (4), where we note that the edge of the optical energy gap for direct transmission increases in all solutions compared to the energy gap optical power in solution DDDW, that the displacement in the energy gap edge can be attributed to the decrease in the size of nanoparticles according to the effect of quantitative confinement. Therefore, the larger energy gap value is suitable for obtaining small size particles [22], the electrons need more energy to move, which happens as the energy gap widens, which is why the increase in E_g is attributed to levels close to the conduction band's electron-filled region [23]. Figure (4) shows direct band gap estimations of colloidal Ag nanoparticles samples.

Table (3): Surface plasmon resonance (SPR) silver nanoparticles.

Nanoparticles Types	Solvent	Absorbance (a.u)	Surface Plasmon Resonance SPR (nm)
$AgNP_s$	DDDW	1.008	400
	SDS	1.014	407
	CTAB	1.222	408
	$NaBH_4$	1.071	415

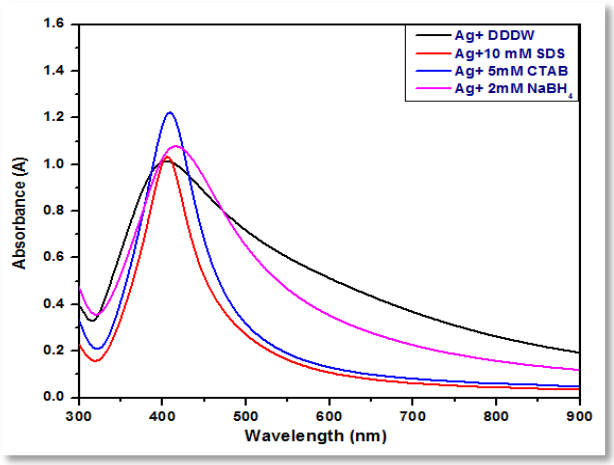

Figure (3): UV-Visible absorption spectra of colloidal Ag nanoparticles.

Table (4): Energy gap values of silver nanoparticles prepared in different solutions.

Solution	Energy Gap (eV)
DDDW	1.76
SDS	2.52
CTAB	2.04
$NaBH_4$	2.08

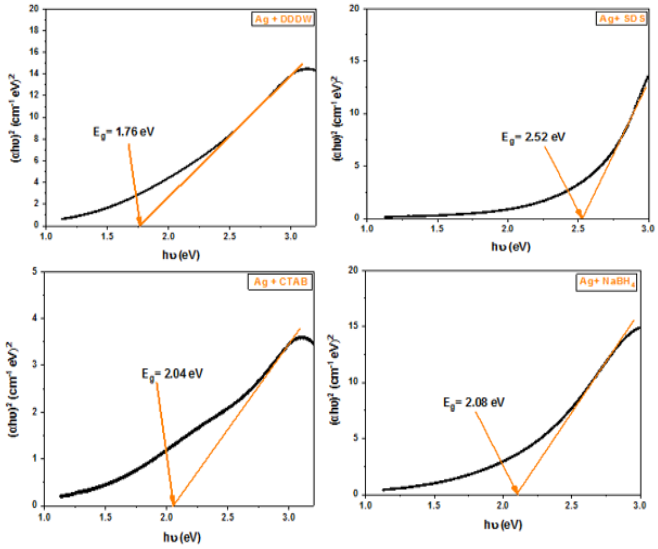

Figure (4): Direct band gap estimations of colloidal Ag nanoparticles samples.

3.2 Transmission Electron Microscopy (TEM) Results

The TEM technique was used to examine the morphological distribution and the statistical size distribution of silver nanoparticles prepared in different liquid environments (DDDW, SDS, CTAB and $NaBH_4$). As shown in table (5) the average size of the particles made in DDDW was 45.718 nm, while silver nanoparticles made in solution $NaBH_4$ were more spread out than those made in DDDW, where the average size of the particles got smaller. TEM images show that $AgNP_s$ form in a spherical shape without sticking together as in figure (5).

Table (5): The average size (nm) values of Ag nanoparticles in different solvent.

Solvent	Average Size (nm)
DDDW	45.718
SDS	50.631
CTAB	48.973
$NaBH_4$	41.198

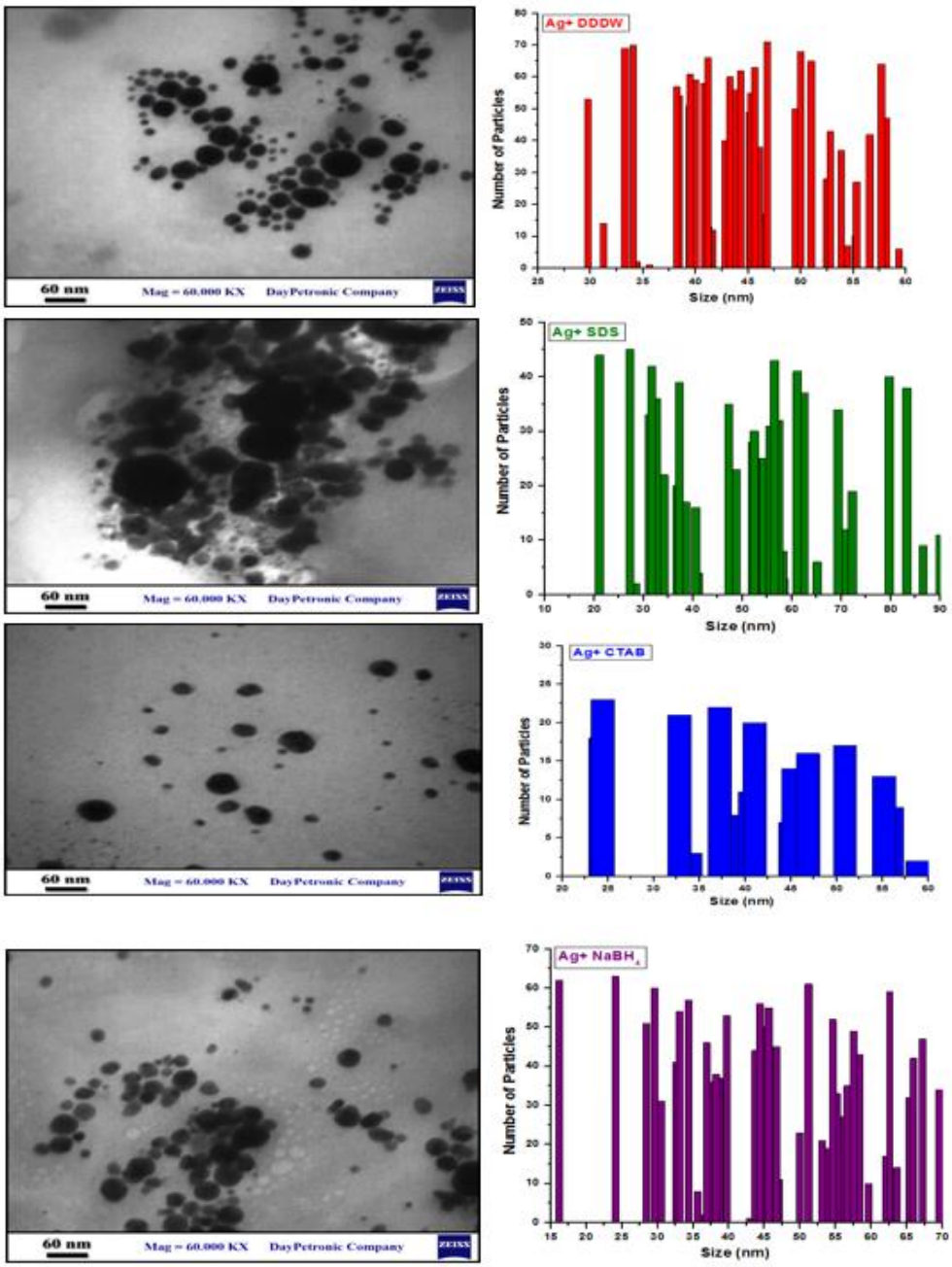

Figure (5): TEM images and histogram of AgNPs colloidal solutions prepared in various solutions (DDDW, SDS, CTAB and $NaBH_4$).

3.3 Antimicrobial Activity of AgNPs

The effectiveness of the prepared metals on viability and activity of *C. albicans* was investigated and the inhibitory effects of the nano-solutions prepared by pulsed laser ablation technique in liquids (PLAL) and prepared in different ionic strength solutions (DDDW, SDS, CTAB and $NaBH_4$) at wavelength (1064nm) energy (500mJ) number of pulses (1000) at different concentrations (0, 25, 50,100 and 200) µg/mL was studied using well diffusion method, from the bellow findings, The effect was exacerbated with increased concentration, and there is a difference among solutions (DDDW, SDS, CTAB and $NaBH_4$) with different concentrations of $AgNP_s$, can be observed that the inhibition rate is increase with raised concentrations of $AgNP_s$, where it is found the (DDDW) and ($NaBH_4$) solutions scored highest inhibition rate (15.60±0.26 and 15.60±0.26) respectively at concentration (200 µg/mL) of $AgNP_s$ compared to (SDS) and (CTAB) solutions that scored least

inhibition rate (11.73±0.12 and 11.17±0.32) at same concentration of AgNPs (200 µg/mL) with significant difference (LSD=0.198). Finally, there is no significant difference among solutions at concentrations of AgNPs (0, 25 µg/mL). As shown in table (6) and figure (6). NP_s exhibited a significant effect against candida viability, and a high growth-inhibiting effect against the diameter of *C. albicans* colonies was observed at high concentrations where there was a statistically significant inhibitory effect at $p \leq 0.05$ of treated cells compared to the control group, as shown in the figure (7). Due to the tiny size of the silver nano particles, they had a greater inhibitory impact on the pathogens of skin illnesses caused by the *C. albicans* than the bulk shape of silver. Because the smallest NP_s have the highest surface area and the strongest antimicrobial effect, reactivity (toxicity) and solubility, which may increase as particle size decreases, will increase dramatically [24]. Silver nanoparticles destroyed ability of candida transformation from yeast-to-hypha, and the extended cells accelerate the candida penetration and potentiate host invasion [25]. The formation of filaments is also required for the development of biofilm colonies. Hyphae provided the structural perfection and multilayered structure for the creation of biofilms [26]. Biofilm-associated cells have lower antifungal sensitivity, which complicates the treatment of fungal infections. Therefore, the suppression of morphological alteration and biofilm formation reduces the pathogenicity of these microorganisms and improves the elimination of the infection. When $AgNP_s$ stick to the surface of a cell, they damage the membrane by sticking to it. This causes structural and functional changes in the membrane, such as the formation of pores and the leakage of cytoplasm. This activity is associated with the release of Ag^{+2} ions from the nanoparticle surface, which induce the formation of reactive oxygen species (ROS) that causes great damage for the essential molecules (proteins, DNA and structural lipids), in addition to that adherent Ag^{+2} ions with microbial outer surfaces, inhibits microbial cell adhesion to host cells, or Ag^{+2} ions disruption of the microenvironment of these pathogens causes a breakdown of the potassium-sodium pump, and inhibits the activity of important enzymes for the colonization.

Table (6): The inhibition zone diameter (mm) of C. albicans at different concentrations of AgNPs.

Concentration µg/mL	DDDW	SDS	CTAB	$NaBH_4$
0	0.0	0.0	0.0	0.0
25	9.67±0.1[a]	0.0	0.0	0.0
50	10.47±0.[illegible]	9.13±0.4[a]	7.23±0.0[illegible]	10.47±0.[illegible]
100	11.87±0.[illegible]	10.10±0.2[illegible]	9.53±0.3[illegible]	11.87±0.[illegible]
200	15.60±0.[illegible]	11.73±0.1[illegible]	11.17±0.[illegible]	15.60±0.[illegible]
LSD CONC.	0.198			

- Each number represent M±SD of three replicate.
- Different letters indicate significant differences at P ≤ 0.05

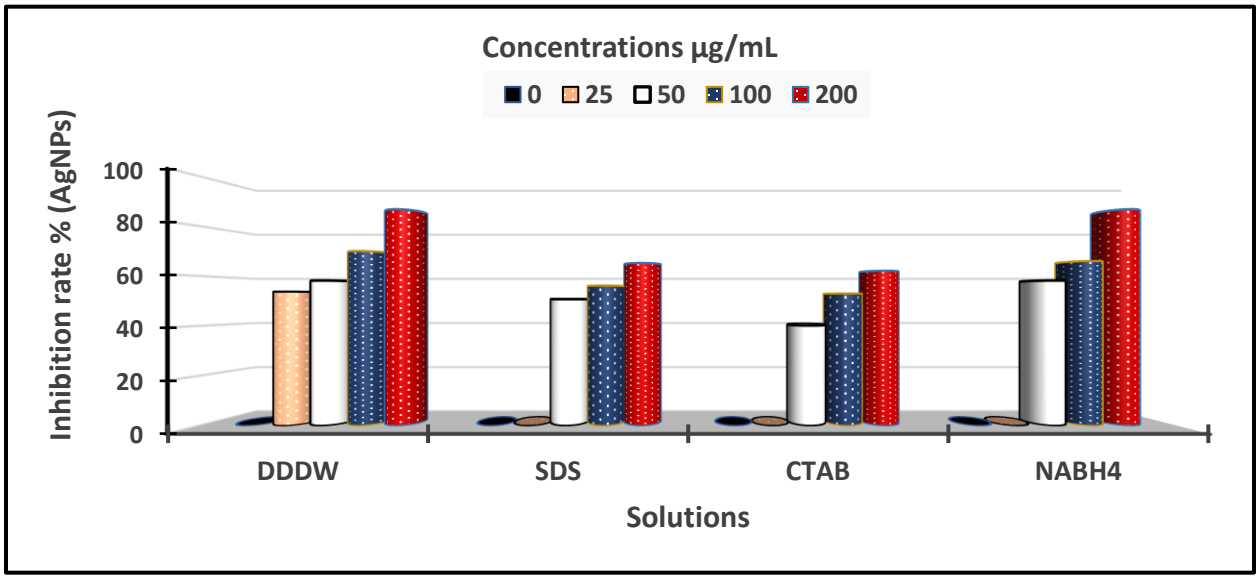

Figure (6): Inhibition rate of C. albicans by using several solutions of AgNPs at various concentrations (0, 25, 50, 100 and 200) µg/ mL.

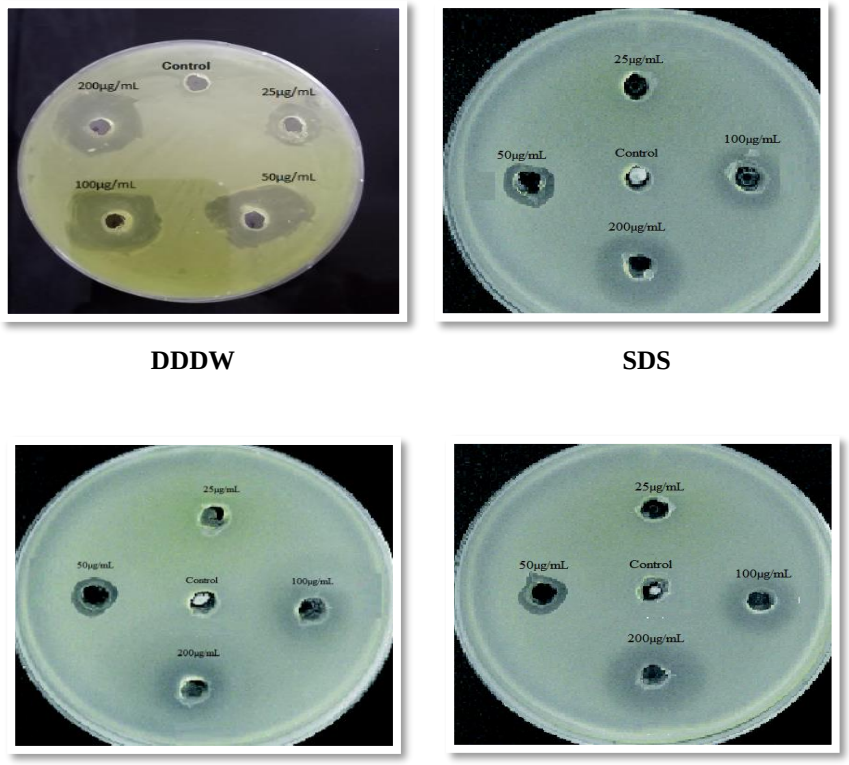

DDDW **SDS**

CTAB NaBH4

Figure (7): Inhibition zone (mm) of C. albicans at different concentrations of AgNPs prepared in different ionic strength solutions.

3.4 Cytotoxic Effects of Prepared AgNPs

Mitotic index (MI) and blastogenic index (BI) are significant bio-indicators for the examination of a variety of chemical and physical parameters due to their sensitivity to such variables and the ability to measure the influence on their occurrence and repetition [27, 28]. From table (7) we can observed decline in the value of each of MI and BI with concentrations′ raising, the significance was apparent in high concentrations more than in low concentrations (P-value 0.453), but there is no significant differences between the two treatments (DDDW and $NaBH_4$) (P- value 0.038). Figure (8) shows some chromosomal aberrations induced by (100µg/mL) of AgNPs prepared in DDDW, because NP_s have unique properties such as specific surface area, high reaction activity, and high penetration effects, they are used in a wide range of industrial and household applications. Because these applications require daily and continuous exposure to such materials, toxicity issues for NP_s have become an essential and inevitable requirement since 2006 [29]. As a result of NP_s interacting with cell structures, large concentrations of metal oxides cause cell cycle changes, resulting in phase delays which explains the decrease in both MI and BI [30]. Ag demonstrated ability to induce cell structure [31].

Table (7): Chromosomal analysis in peripheral blood lymphocytes (PBLs) treated with AgNPs

Concentration µg/mL	AgNPs DDDW			AgNPs $NaBH_4$		
	BI	MI	TCA	BI	MI	TCA
0.0	68.44 ±0.11[a]	1.83± 0.01[a]	0.00	68.44 ±0.12[a]	1.83± 0.02[a]	0.00
25	66.85 ±0.21[a]	1.81± 0.02[a]	0.00[a]	67.85 ±0.22[a]	1.72± 0.04[b]	0.00[a]
50	64.88 ±0.14[a]	1.77± 0.01[a]	0.11± 0.01[b]	67.07 ±0.24[a]	1.68± 0.03[c]	0.11± 0.01[b]
100	63.43 ±0.12[b]	1.65± 0.04[b]	0.15± 0.01[b]	65.23 ±0.31[b]	1.65± 0.01[c]	0.13± 0.01[b]
0.25 MMC	18.21 ±0.22[c]	0.16± 0.01[c]	2.20± 0.01[c]	18.21 ±0.16[c]	0.16± 0.01[d]	2.2±0 .01[c]

- Each number represent M±SD of three replicate.
- Different letters indicate significant differences at P ≤ 0.05.

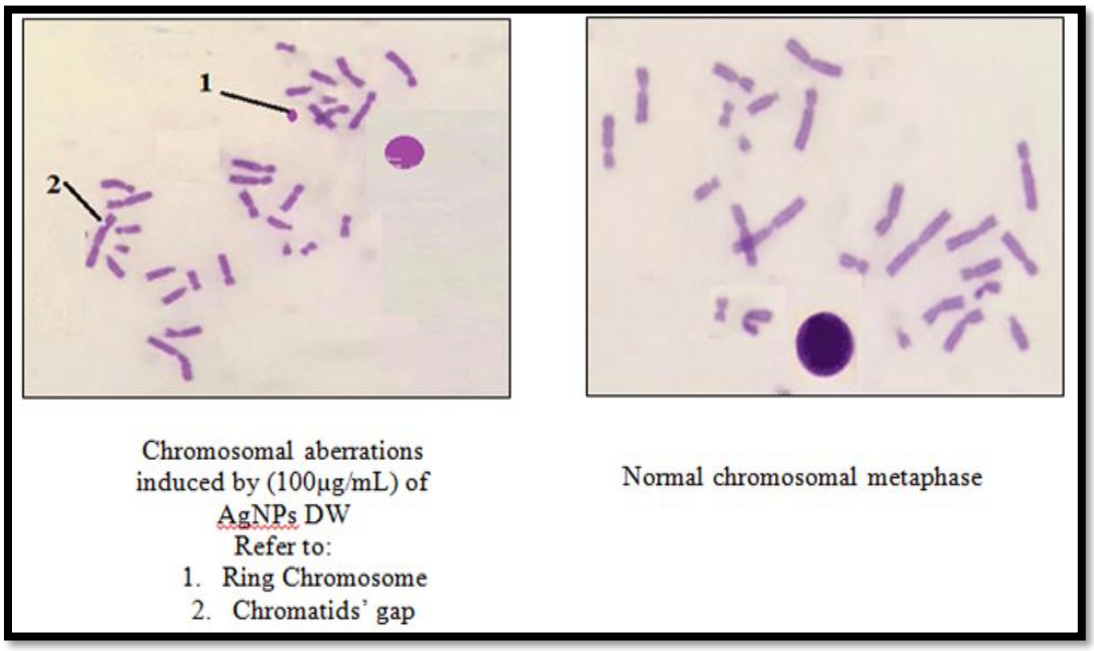

Figure (8): Chromosomal analysis of peripheral blood lymphocytes (PBLs) treated with different concentrations of $AgNP_s$

CONCLUSION

The main conclusion of this study is that pulsed laser ablation in liquids is fast, cheap and good for the environment. UV-VIS and TEM helped show how nanoparticles are made and figure out their size, shape, and other characteristics. These results show that $AgNP_s$ could be a very effective antifungal agent for treating dermatophyte infections caused by fungi. The antifungal activity of $AgNP_s$ against *C. albicans* as a fungicidal model was explored The genotoxicity indicated a decrease in values of (BI) and (MI) with increasing concentrations. While the value of (TCA) only slightly rose because Ag demonstrated ability to induce cell structure.

REFERENCES

J. Simon , H. Y. Sun, H. N. Leong, M. Yvette, C. Barez, P. Huang, D. Talwar, J. H. Wang, M. Mansor, B. Wahjuprajitno, A. Patel, S. Wittayachanyapong, B. S. M. Sany, Sh. F. Lin, G. Dimopoulos, "Echinocandins in Invasive Candidiasis", Mycoses, Vol. 56, pp.601-609, 2013.

M. Dadar, R. Tiwari, K. Karthik, S. Chakraborty, Y. Shahali, K. Dhama, "Candida albicans Biology, Molecular Characterization, Pathogenicity, and Advances in Diagnosis and Control An update", Microbial Pathogenesis, Vol.117, pp.128-138, 2018.

S. S. Gonçalves, A. C. R. Souza, A. Chowdhary, J. F. Meis, A. L. Colombo, "Epidemiology and Molecular Mechanisms of Antifungal Resistance in Candida and Aspergillus", Mycoses Vol. 59, pp. 198-219, 2016.

C. De Bedout and B. L. Gomez, "Candida y Candidiasis Invasora: Un Reto Continuo Parasu Diagnostico Temprano", Infection, Vol. 14, pp. 159-171, 2010.

N. P. De Sa, L. F. F. De Paula, L. F. F. Lopes, L. I. B. Cruz, T. T. S. Matos, C. I. Lino, R. B. Oliveira, E. M. De Souza-Fagundes, B. B. Fuchs, E. Mylonakis, S. Johann, "In Vivo and in Vitro Activity of a Bis-arylidenecyclo-Alkanone against Fluconazole-Susceptible and Resistant Isolates of Candida albicans", The Journal of Global Antimicrobial Resistance, Vol. 14, pp. 287-293, 2018.

V. A. D. Saldana, M. V. Martinez, M. Velazquez, J. R. Sanchez, "Factores De riesgo Y Epidemiologia De la Candidemia en el Hospital Juarez de Mexico", Medicina Interna de Mexico, Vol. 30, pp. 121-132, 2014.

A. K. Ali, "One-Step Synthesis of Copper Oxide Nanoparticles Using Pulsed Laser Ablation in Water: Influence of the Laser Wavelengths on Optical Properties", Engineering and Technology Journal, Vol. 31, pp. 894-902, 2013.

A. K. AL-Ogaili, A.K. Ali and T. H. Ali, "Preparation of Silver Nanoparticles and Study the Optical and Antibacterial Properties," Engineering and Technology Journal, Vol.33, pp. 478-487, 2015.

A. Hamad, L. Li, and Z. Liu, "A Comparison of the Characteristics of Nanosecond, Picosecond and Femtosecond Lasers Generated Ag, TiO2 and Au Nanoparticles in Deionized Water," Applied Physics A, Vol. 120, pp. 1247–1260, 2015.

M. Maciulevicius, A. Vinciunas, M. Brikas, A. Butsen, N. Tarasenka, N. Tarasenko and G. Raciukaitis, "Pulsed-Laser Generation of Gold Nanoparticles with on-Line Surface Plasmon Resonance Detection," Applied Physics A, Vol. 111, pp. 289-295, 2013.

A. Kadhim, A. M. Haleem, R. H. Abbas "Copper Oxide NPs: Synthesis and Their Anti- Dermatophyte Activity against Trichophyton Rubrum" Engineering and Technology Journal, Vol. 35, pp. 276-281, 2017.

D. R. Monteiro, L. F. Gorup, A. S. Takamiya, A. C. Ruvollo-Filho, E. R. De Camargo, D. B. Barbosa, "The Growing Importance of Materials that Prevent Microbial Adhesion: Antimicrobial Effect of Medical Devices Containing Silver", International Journal of Antimicrobial Agents, Vol.34, pp. 103-110, 2009.

M. Rai, A. Yadav, A. Gade, "Silver Nanoparticles as a New Generation of Antimicrobials", Biotechnology Advances, Vol. 27, pp. 76-83, 2009.

D. R. Monteiro, L. F. Gorup, A. S. Takamiya, E. R. De Camargo, A. C. Filho, D. B. Barbosa, "Silver Distribution and Release from an

Antimicrobial Denture Base Resin Containing Silver Colloidal Nanoparticles", J Prosthodont, Vol. 21, PP. 7-15, 2012.

D. B. Warhei, P. J. Borm, C. Hennes, J. Lademann, "Testing Strategies to Establish the Safety of Nanomaterials: Conclusions of an ECETOC Workshop", Inhal Toxicol, Vol.19, pp. 631–643, 2007.

X. Chen, H. J. Schluesener, "Nanosilver: A nanoproduct in Medical Application", Toxicol Lett, Vol. 176, pp. 1–12, 2008.

K. S. Khashan, G. M. Sulaiman, F. A. Abdul Ameer and G. Napolitano, "Synthesis, Characterization and Antibacterial Activity of Colloidal NiO Nanoparticles", Pak. J. Pharm. Sci., Vol.29, pp.541-546, 2016.

R. Verma and A. Babu, "Human Chromosomes: Manual of Basic Techniques, Pregramon Press", New York, 1989.

E. Jawetz, J. I. meluick and E.A. Adelberg, "Review of Medical Micobiology" 14th Ed. Lange California, 2013.

X. Zheng, W. Xu, C. Corredor, S. Xu and J. An, "Laser-Induced Growth of Monodisperse Silver Nanoparticles with Tunable Surface Plasmon Resonance Properties and a Wavelength Self-Limiting Effect", The Journal Physical Chemistry C, Vol. 111, pp. 14962-14967, 2007.

T. Tsuji, D. H. Thang, Y. Okazaki, M. Nakanishi, Y. Tsuboi and M. Tsuji, "Preparation of Silver Nanoparticles by Laser Ablation in Polyvinylpyrrolidone Solution", Applied Surface Science, Vol. 254, pp. 5224-5230, 2008.

S. Dagher, Y. Haik, A. I. Ayesh and N. Tit, "Synthesis and Optical Properties of Colloidal CuO Nanoparticles", Journal of Luminescence, Vol. 151, pp.149-154, 2014.

H. H. Rashed and J. Moatasemballah, "Synthesis and Characterization of Au:CuO Nanocomposite by Laser Soldering on Porous Silicon for Photodetector", Journal of Al-Nahrain University, Vol. 20, pp. 49-59, 2017.

S. K. Misra, A. Dybowska, D. Berhanu, S. N. Luoma and E. V. Jones, "The Complexity of Nanoparticle Dissolution and Its Importance in Nanotoxicological Studies", Science of the Total Environment", Vol. 438, pp.225–232, 2012.

A. D. Dantas, K. K. Lee, I. Raziunaite, K. Schaefer, J. Wagener, B. Yadav and A. R. Gow, "Cell biology of Candida Albicans–Host Interactions", Current Opinion in Microbiology, Vol. 34, pp.111-118, 2016.

H. H. Lara, D. G. Romero-Urbina, C. Pierce, J. L. Lopez-Ribot, M. J. Arellano-Jimenez and M. Jose- Yacaman, " Effect of Silver Nanoparticles on Candida Albicans Biofilms: An Ultra-Structural Study",. J Nano Biotechnology, Vol. 13, pp. 1-12, 2015.

C. Andreoli, P. Leopardi, S. Rossi and R. Crebelli, "Processing of DNA Damage Induced by Hydrogen Peroxide and Methyl Methansulfonate in Human Lymphocytes: Analysis by Alkaline Single Cell gel Electrophoresis and Cytogenetic Methods". Mutagenesis, Vol.14, pp. 497-504, 1999.

G. Gandhi, J. Naru, K. Maninder and K. Gurpreet, "DNA and Chromosomal Damage in Residents Near a Mobile Phone Base Station", Int J Hum Genet, Vol. 14, pp.107-118, 2014.

J. Mytych and M. Wnuk, " Nanoparticle Technology as a Double-Edged Sword: Cytotoxic, Genotoxic and Epigenetic Effects on Living Cells", Journal of Biomaterials and Nanobiotechnology, Vol. 4, pp. 53-63, 2013.

E. Moschini, M. Gualtieri, D. Gallinotti, E. Pezzolato, U. Fascio, M. Camatini and P. Mantecca, " Metal Oxide Nanoparticles Induce Cytotoxic Effects on Human Lung Epithelial Cells A549", Chemical Engineering Transactions, Vol. 22, pp. 29-34, 2010.

X. Hu, S. Cook, P. Wang and H. M. Hwang, "In vitro Evaluation of Cytotoxicity of Engineered Metal Oxide Nanoparticles", Sci Total Environ, Vol. 407, pp. 3070–3072, 2009.